Clinical Immunology 265 (2024) 110287

Contents lists available at ScienceDirect

Clinical Immunology

journal homepage: www.elsevier.com/locate/yclim

Full Length Article

# LL37/self-DNA complexes mediate monocyte reprogramming

Aman Damara [a], Joanna Wegner [a], Emily R. Trzeciak [a], Antonia Kolb [a], Mahsa Nastaranpour [a], Rahul Khatri [a], Andrea Tuettenberg [a,b], Daniela Kramer [a,b], Stephan Grabbe [a,b], Fatemeh Shahneh [a,b,*]

[a] Department of Dermatology, University Medical Center of the Johannes Gutenberg-University of Mainz, Mainz, Germany
[b] Research Center for Immunotherapy, University Medical Center of the Johannes Gutenberg-University of Mainz, Mainz, Germany

ARTICLE INFO

*Keywords:*
Monocyte reprogramming
Metabolic and epigenetic modifications
LL37/self-DNA complex
Psoriasis

ABSTRACT

LL37 alone and in complex with self-DNA triggers inflammatory responses in myeloid cells and plays a crucial role in the development of systemic autoimmune diseases, like psoriasis and systemic lupus erythematosus. We demonstrated that LL37/self-DNA complexes induce long-term metabolic and epigenetic changes in monocytes, enhancing their responsiveness to subsequent stimuli. Monocytes trained with LL37/self-DNA complexes and those derived from psoriatic patients exhibited heightened glycolytic and oxidative phosphorylation rates, elevated release of proinflammatory cytokines, and affected naïve $CD4^+$ T cells. Additionally, KDM6A/B, a demethylase of lysine 27 on histone 3, was upregulated in psoriatic monocytes and monocytes treated with LL37/self-DNA complexes. Inhibition of KDM6A/B reversed the trained immune phenotype by reducing proinflammatory cytokine production, metabolic activity, and the induction of IL-17-producing T cells by LL37/self-DNA-treated monocytes. Our findings highlight the role of LL37/self-DNA-induced innate immune memory in psoriasis pathogenesis, uncovering its impact on monocyte and T cell dynamics.

## 1. Introduction

The innate immune system exhibits the capacity to generate memory immune responses, enabling faster and more robust reactions upon encountering subsequent stimuli, whether identical or unrelated [1]. This phenomenon, termed trained immunity, involves epigenetic and metabolic reprogramming, regulating the gene transcription of monocytes and macrophages [2,3]. Metabolites and intermediates from glycolysis and the tricarboxylic acid (TCA) cycle act as cofactors for epigenetic writers and erasers, inducing monocyte reprogramming by shifting cellular metabolism from oxidative phosphorylation to glycolysis [4–7]. Recent studies indicate that host-derived damage-associated molecular patterns (DAMPs) can induce innate immune memory [8]. Endogenous DAMPs can potentially instigate and amplify a proinflammatory microenvironment in systemic autoinflammatory diseases, such as psoriasis [9], systemic lupus erythematosus (SLE) [10], and type 1 diabetes (T1D) [11,12].

The active form of the human cationic antimicrobial peptide (hCAP18), the 37-amino acid peptide (LL-37) has been shown to upregulate the production of proinflammatory cytokines (IL-1β, IL-6, and IL-8) and chemokines (CXCL1, CCL2, and CCL7) in monocytes [13]. Moreover, LL37 triggers inflammation by enabling immune recognition of endogenous nucleic acids. Studies have demonstrated elevated levels of LL-37, DNA, and RNA in the skin, plasma, and synovial fluids of patients with psoriasis and systemic lupus erythematosus (SLE) compared to healthy individuals. These molecules act as DAMPs and contribute to the development of psoriasis, SLE, and T1D [14,15]. Neutrophils, crucial players in the pathogenesis of psoriasis and SLE [12,16], release high concentrations of LL37, DNA, and RNA during neutrophil extracellular trap (NET) formation at sites of inflammation [9]. Self-DNA alone is degraded immediately by DNases in both intracellular and extracellular environments [11,14]. However, self-DNA, regardless of its nucleotide sequences, can bind to LL37 where it is transported into the cytosol of monocytes, extending its half-life [11,14,17,18], leading to the stable induction of proinflammatory cytokines.

It was shown that the total number of monocytes and the frequency of the intermediate $CD14^{++}CD16^+$ subset increased in the blood of psoriatic patients compared to healthy control individuals [19,20] and contributed to psoriatic inflammation by producing proinflammatory cytokines [21]. Building on this evidence, our hypothesis suggests that LL37/self-DNA trained monocytes undergo reprogramming, supporting monocyte effector functions that may amplify psoriatic inflammation.

* Corresponding author at: Department of Dermatology, University Medical Center of the Johannes Gutenberg-University of Mainz, Mainz, Germany.
*E-mail address:* Fatemeh.Zare-Shahneh@unimedizin-mainz.de (F. Shahneh).

https://doi.org/10.1016/j.clim.2024.110287
Received 16 February 2024; Received in revised form 13 June 2024; Accepted 15 June 2024
Available online 21 June 2024
1521-6616/© 2024 The Authors. Published by Elsevier Inc. This is an open access article under the CC BY license (http://creativecommons.org/licenses/by/4.0/).

This study reveals the role of LL37 bonded to self-DNA, which triggers enhanced responsiveness by epigenetic and metabolic reprogramming of monocytes. Hence, we propose that innate immune memory contributes to psoriasis, prompting an investigation into the proinflammatory phenotype as well as metabolic and epigenetic remodeling of monocytes from naïve patients. Psoriatic peripheral monocytes exhibit enhanced glycolysis and oxidative phosphorylation rates compared to healthy individuals, resembling LL37/self-DNA-trained monocytes. In conclusion, our study sheds light on a different aspect of monocyte reprogramming for the first time, which plays a significant additional role in maintaining systemic inflammation in psoriasis.

## 2. Materials and methods

### 2.1. Reagents

Total human genomic DNA was purchased from Roche (Cat# 11691112001) which was prepared from whole peripheral blood (buffy coat). The synthetic peptide LL37 (Cat# Tlrl-l37–5), TLR2/4 agonist (LPS, Cat# Tlrl-eblps), and TLR7/8 agonist (R848, Resiquimod, Cat# Tlrl-r848) were purchased from InvivoGen. GSK-J4, a selective KDM6A/B inhibitor, was obtained from MedChemExpress (Cat# HY-15648F). Rotenone/antimycin A and 2-deoxy-D-glucose were used from Agilent (Cat# 103346–100). To generate LL37/self-DNA complexes, LL37 (10 μg) was premixed with 2 μg of human genomic DNA (LL37: DNA mass ratio of 5:1) in 10 μl of sterile, endotoxin-free H2O [9,11,14,18] and incubated for 1 h at RT.

### 2.2. Primary cell isolation and culture

Peripheral blood mononuclear cells (PBMC) from healthy donors were obtained with written informed consent with authorization number: 837.019.10 (7028) from the Mainz Blood Bank, Mainz, Germany. PBMC isolation was achieved through differential density centrifugation over Biocoll (Cat# BS-L 6115, Biosell, Berlin, Germany). For the innate memory *in vitro* experiments, monocyte isolation was performed using a hyperosmotic Percoll (Cat# 1003438968, Sigma-Aldrich, St. Louis, USA) density gradient centrifugation (48.5% Percoll, 41.5% sterile $H_2O$, and 0.16 M filter-sterilized NaCl) and washed once with phosphate-buffered saline (PBS). To achieve maximal purity, Percoll-isolated monocytes were left to adhere to polystyrene flat-bottom plates (Corning, NY, USA) for 1 h at 37 °C, 5% $CO_2$ [7,22]. Purified monocytes were cultured in DMEM medium supplemented with 10% fetal calf serum (FCS; ThermoFisher Scientific, Waltham, MA) and 100 μg/ml of penicillin/streptomycin (Cat# C15140–122, Gibco, USA). For trans-well co-culture studies, monocytes were isolated from PBMCs using the MojoSort Human $CD14^+$ Monocyte Isolation Kit (Cat# 480048, BioLegend, San Diego, CA) and $CD4^+$ naïve T cells were purified from PBMCs using the MojoSort Human $CD4^+$ naïve T cell Isolation Kit (Cat# 480042, BioLegend, San Diego, CA). After isolation, cells were washed again in PBS containing 2% fetal calf serum and 1 mmol/L EDTA and cultured in *X-VIVO*-20 medium (Cat# BE04-448Q, Lonza, Belgium).

### 2.3. Psoriasis patient samples

All psoriasis patients (n = 20) were recruited from the Department of Dermatology, University Medical Center Mainz, Germany with no history of any treatments (naïve psoriasis vulgaris patients). Age- and sex-matched healthy donors were included as controls. All participants provided informed written consent, and the study received prior approval from the institutional ethics review board with authorization number: 2019-14135. Patients included both males and females with a median age of 43 and were diagnosed with psoriasis vulgaris based on clinical criteria. Psoriasis Area and Severity Index (PASI) scores ranged from 6 to 37 at the time of enrollment.

### 2.4. Seahorse XFp metabolic flux analysis

For the analysis at 24 h, $5 \times 10^5$ isolated monocytes were seeded and stimulated directly in Seahorse Cell Culture Mini Plates (Cat# 103022–100, Agilent, California, USA). For analysis after day 5 of culture, $1 \times 10^6$ monocytes were cultured in 24-well plates (Greiner, Austria) and stimulated for 24 h. On day 5 of the culture, $1 \times 10^5$ cells were seeded in Mini Plates. Analysis was performed in DMEM with 0.6 mM glutamine, 5 mM glucose, and 1 mM pyruvate, pH 7.4. Cells were left to rest in a non-$CO_2$ incubator at 37 °C for 1 h. Oxygen consumption rates (OCR) and extracellular acidification rates (ECAR) were measured using a Cell Mito Stress Test Kit in a Seahorse XFp Analyzer in accordance with the recommendations by the manufacturer (Cat# 103010–100, Agilent, California, USA). The final concentrations of applied inhibitors are as follows 2 μM oligomycin, 1 μM FCCP, and 0.5 μM rotenone/antimycin A.

### 2.5. Cytokine quantification and ELISA

Production of IL-6, IL-8, IL-23, and TNF-α was measured in supernatants using the following commercial Max Deluxe Set ELISA kits: IL-6 (Cat# 430504), IL-8 (Cat# 431504), TNF-α (Cat# 430204), IL-23 (Cat# 437607) from BioLegend. The level of LL-37 and TGF-β1 was measured in supernatants using a Human LL-37 ELISA Kit (Cat# NBP3–06932) from NOVUS Biologicals and DuoSet Human TGF-β1 (Cat# DY240–05) from R&D systems following the instructions of the manufacturer.

### 2.6. KDM6A/B enzymatic activity

The isolation of nuclear proteins from the cells was carried out using the Nuclear Extraction Kit (Cat# Ab113474, Abcam, Cambridge, United Kingdom), followed by protein concentration determination using the Pierce™ BCA protein assay kit (Cat# 23225, Thermo Fisher Scientific, MA, USA). The assessment of KDM6A/B enzyme activity was conducted on 1 μg of nuclear extract using the KDM6A/KDM6B Activity Quantification Assay Kit (Cat# ab156911, Abcam), following the manufacturer's instructions.

### 2.7. Chromatin immunoprecipitation (ChIP) analysis

Monocytes were fixed with 1% formaldehyde (Cat# 28908, Thermo Scientific) after 24 h stimulation with LL37/self-DNA and sonicated. 1 mg of fixed and sonicated chromatin DNA was immunoprecipitated using 1 μg of H3K4me3 (Cat# C15410003, Diagenode) or H3K27me3 antibodies (Cat# C15410195, Diagenode). Normal rabbit IgG from the kit served as the control immunoprecipitation (IP) antibody. ChIP was performed according to the manufacturer's instructions (Pierce Magnetic ChIP Kit, Cat# 26157, Thermo Scientific). For qPCR analysis, IL-6, IL-8, and TNF-α promoter primer pairs were employed and the 2-ΔΔCt method was used with normalized samples using input DNA. Data is represented as the percentage of input DNA. Primers used for qPCR analysis are as follows: *TNF*_F: CACATACTGACCCACGGCTC, *TNF*_R: AGAGGCTGAGGAACAAGCAC, *IL6*_F: AGGGAGAGCCAGAACACAGA, *IL6*_R: GAGTTTCCTCTGACTCCATCG, *IL8*_F: ACTGAGAGTGATTGAGAGTGGAC, *IL8*_R: AACCCTCTGCACCCAGTTTTC, *H2B*_F: TGTACTTGGTGACGGCCTTA, *H2B*_R: CATTACAACAAGCGCTCGAC *Myoglobulin_F*: AGCATGGTGCCACTGTGCT, and *Myoglobulin_R*: GGCTTAATCTCTGCCTCATGAT.

### 2.8. RNA isolation and RT-PCR

Total RNA extraction was performed using the PureLink RNA Mini Kit (Cat# 12183025, Thermo Scientific) following the manufacturer's instructions. RNA concentrations were determined using Nanodrop software. Subsequently, cDNA was synthesized using Syber Green qPCR Master Mix Universal (Cat# HY-K0501A, MedChemExpress). Relative

mRNA expression levels were compared to non-primed and non-stimulated samples, serving as references. Primers used for qPCR analysis are as follows: *IL17A*_F: AAGGTCCTCAGATTACTACAACCG, *IL17A*_R: ATCTCTCAGGGTCCTCATTGCG, *IL17F*_F: TCACGTAACATCGAGAGCCG, *IL17F*_R: GAGCATTGATGCAGCCCAAG, *RORC*_F: GTGGGGACAAGTCGTCTGG, and *RORC*_R: AGTGCTGGCATCGGTTTCG. Gene expression levels were normalized to the *RLP13*_F: CCTGGAGGAGAAGAGGAAAGAGA and *RLP13*_R: TTGAGGACCTCTGTGTATTTGTCAA housekeeping gene and presented as fold changes employing the 2-ΔΔCt method.

### 2.9. Monocyte-T cell trans-well culture and cytokine assays

Purified $CD14^+$ monocytes were loaded into 100 μl trans-well inserts (using polycarbonate, 24 well plates, 0.4 μm pore size, Cat# 1015595, Corning) and stimulated with/without LL37/self-DNA. In the lower chamber, isolated $CD4^+$ naïve T cells were seeded at a 1:4 ratio (25% T cells/75% monocytes) [23,24] in the presence of 1 μg/ml soluble anti-CD3 mAb (Cat# 317302, BioLegend, San Diego, CA) and anti-CD28 mAb (Cat# 302902, BioLegend, San Diego, CA). Cells were cultured in X-VIVO-20 medium supplemented with 1% Penicillin/Streptomycin, 1% Glutamine, and 10% heat-inactivated serum. As controls, naïve $CD4^+$ T cells were activated with anti-CD3/CD28 antibodies without the addition of LL37/self-DNA. At the same time, T cells were activated with anti-CD3/CD28 antibodies and cultured without monocytes in the presence of LL37/self-DNA. Purified $CD14^+$ monocytes isolated from psoriasis patients (Pso) were loaded into 100 μl trans-well inserts and stimulated with or without LPS. In the lower chamber, isolated $CD4^+$ naive T cells from healthy donors (HD) were seeded at a 1:4 ratio in the presence of 1 μg/ml soluble anti-CD3 monoclonal antibody (mAb) and anti-CD28 mAb. As controls, naive $CD4^+$ T cells were activated with anti-CD3/CD28 antibodies alongside monocytes from HD.

The relative levels of 105 selected cytokines and chemokines in supernatants of LL37-self DNA-treated monocytes-T cells and T cells alone were analyzed by the Proteome Profiler Human XL Cytokine Array Kit (Cat# ARY022B, R&D Systems, Wiesbaden, Germany) according to the manufacturer's instructions. Array pictures were captured and analyzed with Fiji ImageJ software.

### 2.10. Flow cytometry analysis

Single-cell suspensions were pre-treated with unlabeled monoclonal antibodies against CD16/CD32 (Cat# 553141, clone 2.4G2, BD Biosciences) to block nonspecific Fc receptor-mediated binding. Subsequently, cells were stained at 4 °C for 30 min with fixable viability dye (Cat# 65–0865-14, Invitrogen, Waltham, MA, USA), followed by the surface and intracellular staining with fluorochrome-conjugated antibodies. Monocytes were stained with surface antibodies such as HLA-DR (Cat# 307650, clone L243, dilution 1:100, BV650, BioLegend), CD14 (Cat# 325618, clone HCD14, dilution 1:200, PE-Cy7, BioLegend), and CD16 (Cat# 302038, clone 3G8, dilution 1:100, BV421, BioLegend). NK cells, B cells and T cells were excluded by staining with anti-CD56 (Cat# 318340, clone HCD56, dilution 1:200, BV510, BioLegend), anti-CD19 (Cat# 302242, clone HIB19, dilution 1:200, BV510, BioLegend) and anti-CD3 (Cat# 317332, clone OKT3, dilution 1:200, BV510, BioLegend) antibodies.

After surface staining, cells were fixed and permeabilized using eBioSciences Foxp3/Transcription Factor Buffer Set (Invitrogen, 5523) and stained with anti-pSTAT3 (pY705) (Cat# 612569, clone: 4/P-STAT3, dilution 1:200, PE, BD Bioscience), anti-NF-κB p65 (Cat# 653006, clone 14G10A21, dilution 1:50, PE, BioLegend), and isotype control (Cat# 558595, clone: MOPC-173, dilution 1:200, PE, BD Bioscience). H3K27me3 and H3K4me3 were measured using Tri-Methyl-Histone H3 (Lys27) rabbit mAb (Cat# 12158, dilution 1:50, Alexa Fluor 647, Cell Signaling Technology) and Tri-Methyl-Histone H3 (Lys4) rabbit mAb (Cat# 62255, dilution 1:50, PE Cell Signaling Technology).

For intracellular staining and the measurement of intracellular IL-17 production, previously stimulated $CD4^+$ T cells were restimulated for 5 h with 2 μl cell activation cocktail with brefeldin A (Cat# 423303, BioLegend, San Diego, CA). Cells were stained with antibodies CD3 (Cat# 345763, clone SK7, dilution 1:100, BD Bioscience), CD4 (Cat# 348809, clone SK3, dilution 1:100, BD Bioscience), fixed and permeabilized using BD Cytofix/Cytoperm (Cat# 555028, BD Bioscience, Heidelberg, Germany), followed by staining with anti-IL-17A antibodies (Cat# 512306, clone BL168, dilution 1:80, PE, BioLegend).

To measure reactive oxygen species (ROS), the CellRox Kit (Cat# C10492, Thermo Fisher Scientific) was used according to the manufacturer's instructions. The CellRox detection reagent was added directly to the 24 h and 4 days rested LL37/self-DNA-trained monocytes and incubated for 30 min at 37 °C, 5% $CO_2$ in the dark. Unstained cells as well as cells treated with TBHP (tert-butyl hydroperoxide), were used as negative and positive controls.

All flow cytometry measurements were performed on a BD LSR II (Becton Dickinson, Heidelberg, Germany). Flow Jo Version 10 was used for data analysis. Doublet, debris, and dead cells were excluded from the analysis. Example gating strategies of monocyte subsets examined in this study can be found in Fig. S1A.

### 2.11. Western blot analysis

Monocytes were washed in PBS and resuspended in lysis buffer containing 20 mM TRIS-HCl pH 7.5, 150 mM NaCl, 1% Triton X-100, 1 mM $Na_2EDTA$, 1 mM EGTA, 1 mM β-glycerophosphate, 2 M urea and 1× protease inhibitor cocktail (Cat# P8465, Sigma-Aldrich). After 10 min on ice, samples were briefly sonicated to disrupt DNA–protein complexes. Afterwards samples were separated by SDS-PAGE and transferred to a nitrocellulose membrane. Membranes were incubated with antibodies against H3K4me3 (Cat# C15410003, dilution 1:1000, Diagonade), H3K27me3 (Cat# 9733, dilution 1:1000, Cell Signaling), histone H3 (Cat# ab1791, dilution 1:2000, Abcam), pSTAT3 (Y705) (Cat# 9145, dilution 1:500, Cell Signaling), STAT3 (Cat# 4904, dilution 1:1000, Cell Signaling), pIκBα (S32) (Cat# 2859, dilution 1:500, Cell Signaling), IκBα (Cat# 9242, dilution 1:1000, Cell Signaling), and β-actin (Cat# 3700, dilution 1:1000, Cell Signaling) for western blot analysis.

### 2.12. Statistical analysis

The sample size, number of replicates, and detailed statistical information for each experiment are provided in the figure legends. All data are presented as mean ± SEM, as specified in the respective figure legends unless otherwise stated. For comparison between the two groups, the Mann–Whitney *U* test was performed. For comparison between more than two groups, one-way ANOVA followed by Dunnett's multiple comparisons test was used. For comparisons where we had two independent variables, two-way ANOVA followed by Sidak's multiple comparisons test was used. Significance was evaluated by the above-mentioned tests and was performed in GraphPad Prism (v6).

## 3. Results

### 3.1. LL37/self-DNA complexes enhance monocyte responsiveness and alter metabolic activity in healthy donors (HD)

Employing a well-established *in vitro* two-hit monocyte model of trained immunity [7,22], we assessed the induction of innate immune memory by LL37 alone or LL37/self DNA stimulation. Healthy donor (HD) monocytes were exposed to LL37 (10 μg/ml) and LL37/self-DNA (20 μg/ml) for 24 h, followed by a rest period in fresh medium for 4–5 days without further stimulation. Subsequently, these monocyte-macrophages encountered a secondary stimulus involving the TLR4

agonist LPS (10 ng/ml) and the TLR7/8 agonist R848 (1 μg/ml) (Fig. 1A). On day 5, pre-conditioned HD monocytes displayed elevated release of the proinflammatory cytokines, IL-8, IL-6, and TNF-α (Fig. 1B), upon restimulation, indicative of trained immunity. As shown previously [11,14], DNA alone did not trigger the activation of these proinflammatory cytokines (Fig. S1B) and LL37 alone induced weaker activation of IL-8 and TNF-α compared to LL37/self-DNA treatment (Fig. 1B). Since it was shown that monocytes steadily internalize LL37/self-DNA complexes (but not DNA alone) immediately after treatment *via* CXCR2-specific endocytosis [11], we evaluated the production of the elevated proinflammatory cytokines in the rested HD monocyte before the second stimulation (trained HD monocytes). The release of IL-8 and TNF-α cytokines demonstrated an upward trend during resting periods compared to the 24 h stimulation with LL37/self-DNA complexes (Fig. 1C).

The connection between epigenomic alterations and metabolic modifications in monocytes forms a basis of the trained immunity paradigm [2,25,26]. Our investigation, using a model of innate immune

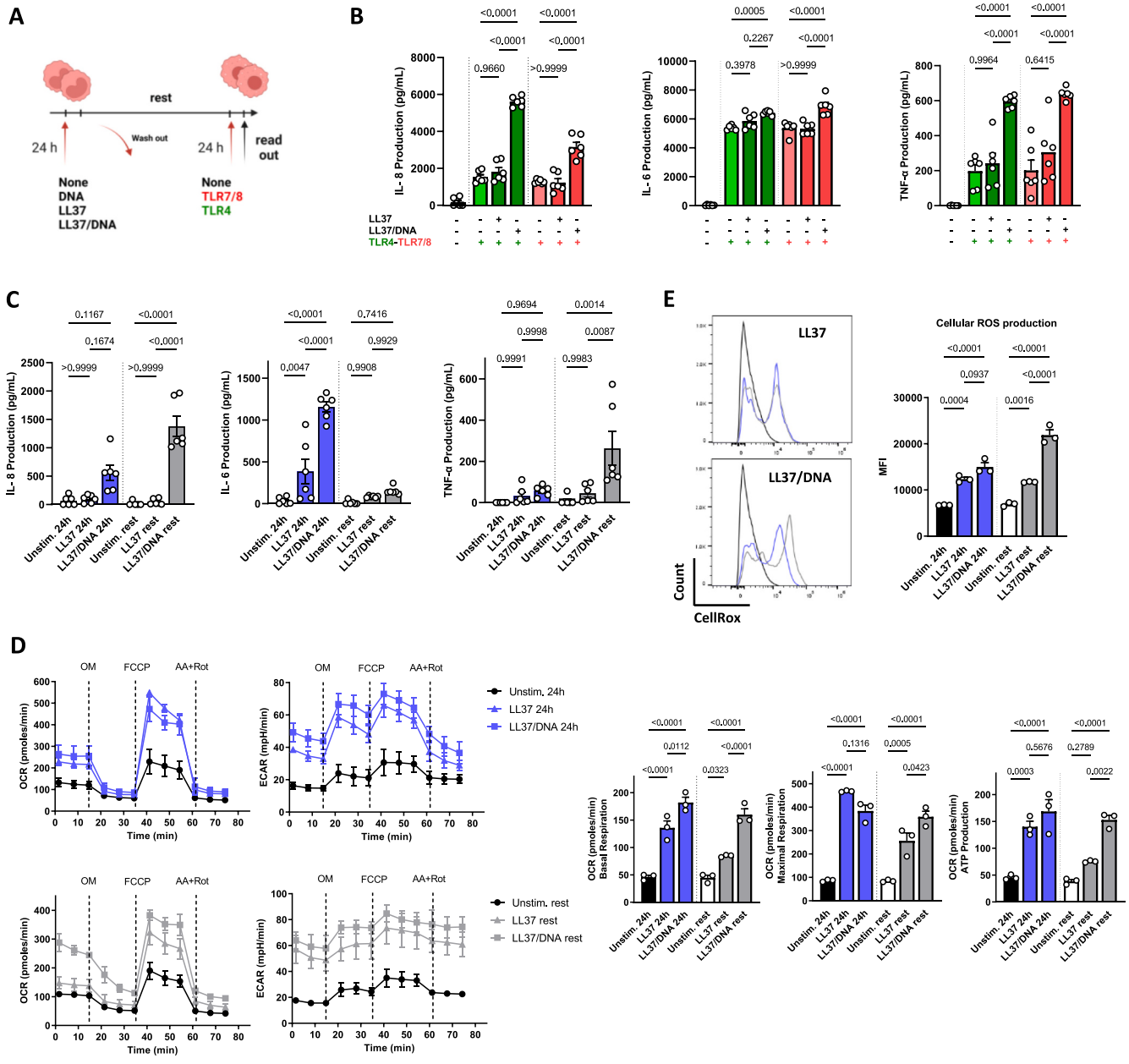


**Fig. 1.** Enhanced IL-8, IL-6, and TNF-α production, metabolic activities, and ROS production in LL37 alone and LL37/self-DNA-treated HD monocytes. (A) Schematic representation of the *in vitro* training model. HD monocytes were treated with LL37 alone or LL37/self-DNA complexes for 24 h, followed by a resting period of 4–5 days, then re-stimulated with TLR4 and TLR7/8 agonists for 24 h. (B) The production of IL-8, IL-6, and TNF-α were quantified by ELISA in cell supernatants of the HD monocytes treated with LL37 alone and LL37/self-DNA complexes (n = 5). (C) The levels of IL-8, IL-6, and TNF-α were measured at 24 h and 4 days after the initial stimulation with LL37 alone and LL37/self-DNA (n = 5). (D) Oxygen Consumption Rates (OCR) and Extracellular Acidification Rates (ECAR) in LL37 alone and LL37/self-DNA-treated HD monocytes were assessed 24 h and 4 days after the initial stimulation. OM: oligomycin and AA+Rot: Antimycin A. + Rotenone. Mean basal and maximal OCR levels and the mean of ATP production rate derived from mitochondrial and glycolytic pathways in LL37 alone and LL37/self-DNA-treated HD monocytes at 24 h and 4 days post the initial stimulation (n = 3). (E) ROS generation in LL37 alone and LL37/self-DNA-treated HD monocytes at 24 h and 4 days following the first stimulation (n = 3). (Error bars show means ± SEM, *P* values were calculated using one-way ANOVA followed by Dunnett's multiple comparisons test.).

memory, uncovered a pivotal role of LL37 alone and LL37/self-DNA complexes in modulating the metabolic activity of HD monocytes. We observed a distinct shift in metabolic behavior, characterized by a significant elevation in mitochondrial oxidative phosphorylation (OXPHOS) and glycolytic rates, as shown by enhanced oxygen consumption rate (OCR) and extracellular acidification rates (ECAR) (Fig. 1D). This increase in aerobic glycolysis is akin to the Warburg effect. Interestingly, although trained HD monocytes were left unstimulated before the secondary challenge on day 4 of rest, the heightened glycolytic activity persisted, indicating an enduring alteration in the metabolic profile that did not revert to the baseline metabolic state (Fig. 1D). This increased extracellular acidification rate in trained HD monocytes suggested lactate accumulation due to enhanced aerobic glycolysis. Notably, trained HD monocytes displayed elevated ATP

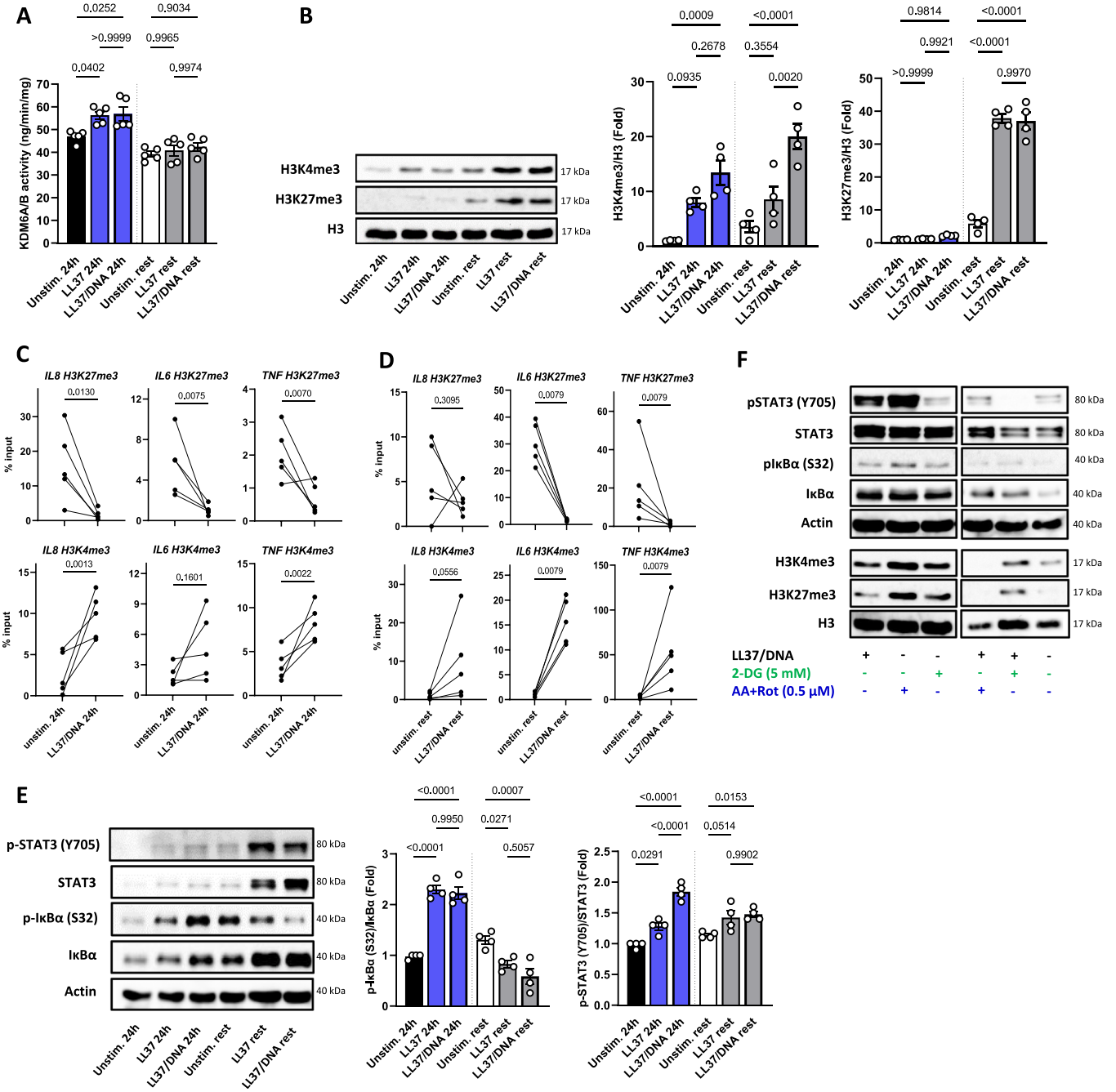


**Fig. 2.** LL37 alone and LL37/self-DNA-mediated epigenetic modifications and associated signaling in HD monocytes. (A) Assessment of KDM6A/B enzymatic activity in HD monocytes 24 h and 4 days post-initial stimulation with LL37 alone and LL37/self-DNA complexes by ELISA (n = 5). (B) Western blot analysis depicting H3K27me3 and H3K4me3 marks in HD monocytes treated with LL37 alone and LL37/self-DNA complex for 24 h and following 4 days' rest (n = 4). (C) Comparison of epigenetic modifications in LL37/self-DNA-treated HD monocytes, demonstrating significantly decreased H3K27me3 marks and increased H3K4me3 marks at the promoter regions of *IL6*, *IL8*, and *TNF* genes compared to untreated HD monocytes 24 h and (D) 4 days post-initial stimulation (n = 5). (E) Western blot analysis depicting activation p-STAT3, STAT3, p-IκB-α and IκB-α in HD monocytes treated with LL37 alone and LL37/self-DNA complexes for 24 h and 4 days of rest (n = 4). (F) Western blot analysis of HD monocytes from untreated or treated with LL37/self-DNA complexes for 24 h in the presence of 2-DG or AA (Antimycin A) and Rot (Rotenone) inhibitors (Error bars show means ± SEM, P values were calculated using Wilcoxon signed rank test and one-way ANOVA followed by Dunnett's multiple comparisons test.).

generation and heightened basal and maximal respiration in a mitochondria-dependent manner, signifying an enhanced metabolic state compared to unstimulated counterparts (Fig. 1D). The concurrent elevation in glycolysis and oxidative phosphorylation implies that LL37/self-DNA and in a lesser extent, LL37 alone stimulation can reprogram the long-term metabolic activities of HD monocytes by simultaneously boosting both glycolytic and mitochondrial metabolic rates.

Given the role of mitochondrial metabolism and ATP production in driving reactive oxygen species (ROS) generation, a critical factor in promoting proinflammatory cytokine production essential for trained immunity [3], we quantified ROS levels. We found that the LL37/self-DNA complexes and LL37 alone significantly increased ROS production capacity after 24 h stimulation or the resting period (Fig. 1E). Collectively, LL37/self-DNA-induced adaptations in HD monocytes are associated with an innate memory immune phenotype characterized by increased monocyte responsiveness and reprogramming of metabolic activities.

### 3.2. LL37/self-DNA complex training is accompanied by epigenetic reprogramming and is mediated via the STAT3-NF-κB activation pathway

Establishing a long-lasting responsive phenotype in trained HD monocytes is closely tied to epigenomic reprogramming [25]. At the molecular level, trained immunity is intricately linked with histone modifications, particularly histone H3 lysine 4 methylation (H3K4me3) and histone H3 lysine 27 methylation (H3K27me3), which subsequently influence transcription [27]. To study the potential histone modifications post-treatment with LL37 alone and LL37/self-DNA complexes, we analyzed the enzymatic activity of the histone demethylases KDM6A/B, which remove repressive H3K27me3 marks and the global levels of H3K27me3 and H3K4me3. Following stimulation with LL37 alone and LL37/self-DNA complexes, HD monocytes exhibited a significant upregulation in KDM6A/B enzymatic activity within 24 h, which returned to the baseline of unstimulated state at day 4 of rest (Fig. 2A). Subsequent western blot analysis displayed increased global H3K4me3 marks after 24 h of LL37 alone and LL37/self-DNA complexes stimulation, with increased protein levels in both marks in the resting trained HD monocytes (Fig. 2B). Chromatin immunoprecipitation PCR uncovered enriched deposition of the histone H3K4me3 mark and reduced deposition of the H3K27me3 mark at the promoter regions of genes of *IL6, IL8,* and *TNF* after stimulation of HD monocytes with LL37 alone (Fig. S2) and LL37/self-DNA complexes (Fig. 2C) within 24 h, as well as in the resting trained HD monocytes (Fig. 2D and Fig. S2). These epigenomic alterations suggest a poised transcriptional state for *IL6* and *TNF* genes. This insight highlights how LL37 alone and LL37/self-DNA complexes orchestrate epigenomic modulation, enhancing the activity of specific enzymes and leading to higher histone H3K4me3 and lower histone H3K27me3 marks at critical promoter regions such as *IL6* and *TNF*, resembling changes elicited by typical inducers of innate memory. However, genome-wide profile mapping of H3K4me3 and H3K27me3 is needed to understand which further gene activations and repressions are associated with monocyte reprogramming induced by LL37/self-DNA complex activation or training.

Studies indicate NF-κB and STAT3 transcription factors are pivotal in proinflammatory cytokine production and chronic inflammation [28,29]. KDM6B, activated by STAT3, enhances proinflammatory gene transcription *via* the JAK2/STAT3 pathway [30]. KDM6A/B's activity in removing H3K27me3 and recruiting p65 regulates IL-6 and TNF-α production in LPS-activated monocytes, exacerbating inflammation [31,32]. Moreover, NF-κB induces KDM6A/B in monocytes and macrophages in response to inflammatory stimuli [29].

To investigate the signaling cascade that modifies HD monocyte activities during innate immune memory, we analyzed STAT3 and NF-κB pathway alterations in HD monocytes treated with LL37 alone and LL37/self-DNA complexes. As shown in Fig. 2E, both LL37 alone and LL37/self-DNA complexes were associated with high expression of phospho-IκB-α (p-IκB-α) compared to the unstimulated state after 24 h of stimulation. Furthermore, the induced phosphorylation of STAT3 after 24 h of stimulation and strong upregulation in the rested trained groups, suggested that the inflammatory response caused by LL37 alone and LL37/self-DNA complexes was linked to the STAT3-NF-κB pathway. These results suggest the influence of LL37 alone and LL37/self-DNA complexes within the NF-κB-STAT3 signaling axis, enhance the expression of NF-κB-STAT3-related proinflammatory genes by modulating the transcription of IL-8, IL-6, and TNF-α, resulting in heightened responsiveness.

Since we observed stronger activities after LL37/self-DNA treatments, we evaluated the importance of glycolysis for LL37/self-DNA-activated HD monocytes within the NF-κB-STAT3 signaling axis. We blocked or induced the glycolysis for 24 h during LL37/self-DNA stimulation. Glycolysis was inhibited with 5 mM of 2-deoxy-D-glucose (2-DG), a glucose analog, and induced with 500 nM of complex I (Rotenone) and complex III (Antimycin A) inhibitors (AA+Rot). Inhibition of glycolysis with 2-DG resulted in a downregulation of STAT3 activation and the protein level of IκB-α in LL37/self-DNA-treated HD monocytes compared to the unstimulated group (Fig. 2F), demonstrating the relationship between glycolysis and STAT3-NF-κB activation in LL37/self-DNA-treated HD monocytes for 24 h. Finally, the induction of compensatory glycolysis by blocking mitochondrial respiration with AA+Rot decreased the H3K27me3 protein level in LL37/self-DNA-treated HD monocytes compared to the unstimulated and control groups (Fig. 2F).

Although it has been shown that STAT3 inhibition leads to the upregulation of KDM6B and that STAT3 binds to the KDM6B promoter [33], further protein-protein interaction studies are needed to identify direct interactions between KDM6A/B and non-histone proteins in the STAT3 and NF-κB activation pathways.

### 3.3. Increased glycolysis and OXPHOS in psoriatic monocytes

Golden et al. showed that the total number of monocytes and frequency of the intermediate $CD14^{++}CD16^{+}$ subset are increased in the blood of psoriatic patients compared with healthy control individuals [19]. Consistent with these findings, we observed an increased frequency of intermediate monocytes ($CD14^{++}CD16^{+}$) in the blood of naïve psoriatic patients, contributing to psoriatic inflammation by producing psoriatic cytokines (Fig. 3A) [34]. Given the elevated levels of LL-37 in the plasma of naïve psoriasis patients (Fig. 3B), increased KDM6A/B activities in psoriatic (Pso) monocytes at baseline, and the pivotal role of LL37 and LL37/self-DNA complexes in psoriasis pathology [18], we investigated whether the metabolic activities of Pso monocytes differ from those of healthy donor (HD) controls at baseline *ex vivo.* Unexpectedly, we found that Pso monocytes isolated from the blood of psoriatic patients exhibited heightened levels of both OXPHOS and glycolysis (Fig. 3C), similar to LL37 alone and LL37/self-DNA-treated HD monocytes after the rest period. Notably, cytokine production, including IL-8, IL-6, and TNF-α, showed significant elevation in Pso monocytes at baseline and upon stimulation with TLR7/8 and TLR4 ligands compared to those from HD controls after 24 h (Fig. 3D). Subsequent flow cytometric analysis displayed increased global levels of H3K4me3 marks, pSTAT3, and NF-κB p65 in Pso monocytes compared to HD controls at baseline (Fig. 3E).

Previous studies have revealed elevated levels of circulating $IL\text{-}17A^{+}$ $IFN\text{-}\gamma^{-}$ $CD4^{+}$ cells in untreated psoriatic patients [35]. Given that interactions between monocytes and CD4+ T cells are implicated in the severity of several autoimmune diseases [23,35], we investigated the effect of Pso monocytes *via* secreted soluble factors on naïve HD peripheral blood $CD4^{+}$ T cells (Fig. 3F Pso and HD monocytes were stimulated with or without LPS (10 ng/ml) within trans-well plate inserts and co-cultured with naïve $CD4^{+}$ T cells at a 25:75 T cells/monocytes ratio (Fig. S3A) [23,24]. After 24 h of culture, the top inserts containing monocytes were removed, and the HD $CD4^{+}$ T cells were analyzed after

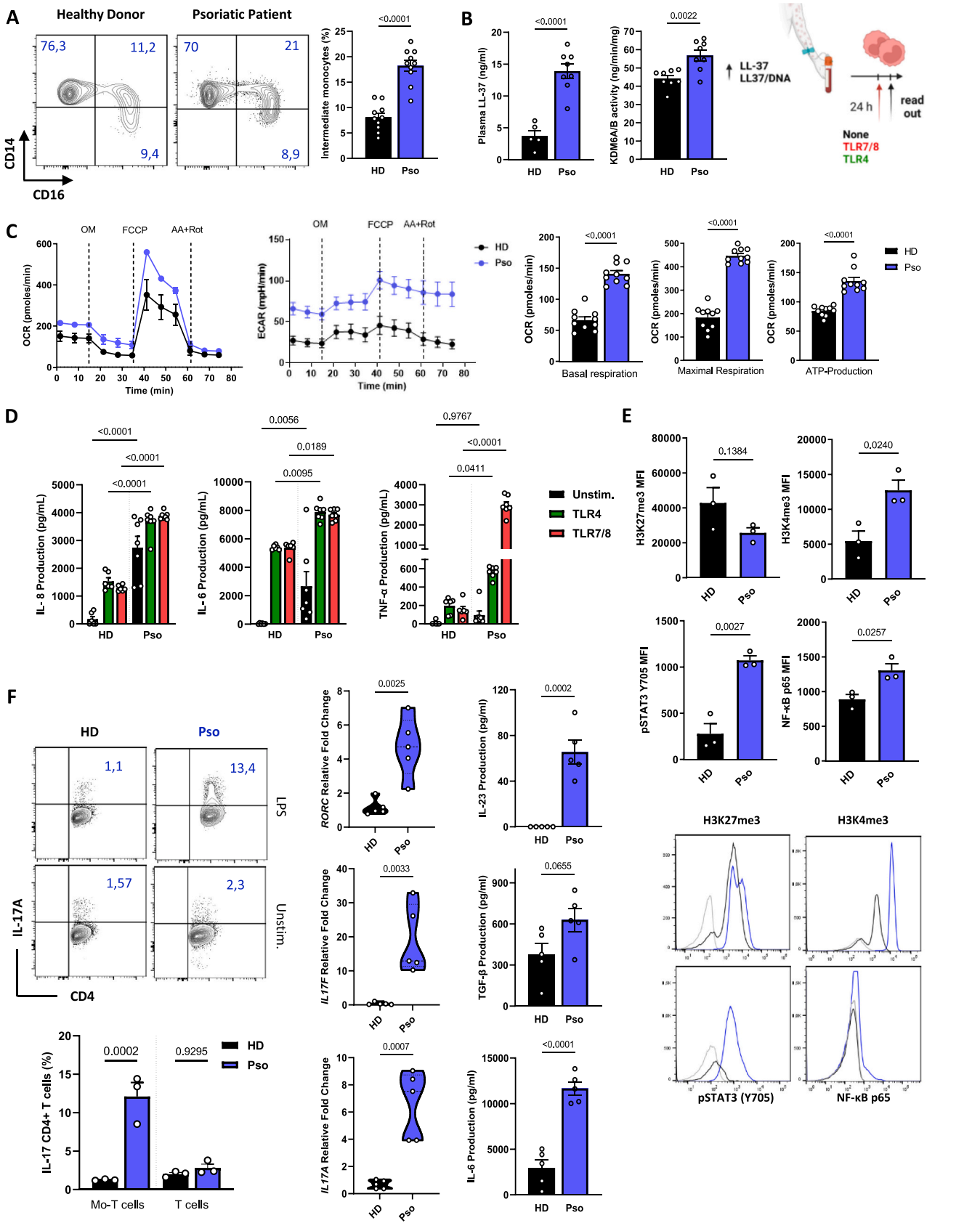


*(caption on next page)*

**Fig. 3.** Evaluation of trained immunity phenotype in psoriatic monocytes. (A) Representative flow plots and the percentage of intermediate ($CD14^{++}CD16^{+}$) monocytes analyzed in naïve psoriatic (Pso) by flow cytometry (n = 10) when compared with healthy donors (HD) (n = 10). (B) Schematic representation of the *ex vivo* model. The level of LL37 in the plasma of naïve Pso patients (n = 8) compared to HD (n = 5) measured by ELISA. Assessment of KDM6A/B enzymatic activity in Pso monocytes at baseline levels compared to HD monocytes measured by ELISA (n = 8). (C) OCR and ECAR between Pso and HD monocytes under basal conditions. Data represents findings from 10 naïve psoriatic patients. (D) Naïve Pso and HD individual monocytes were exposed to TLR7/8 and TLR4 ligands for 24 h. Subsequently, the production levels of IL-6, IL-8, and TNF-α, in cell supernatants were quantified by ELISA (n = 6–7). (E) Flow cytometry analysis depicting the activation of p-STAT3 and NF-κB p65 in Pso monocytes compared to HD monocytes under basal conditions (n = 3). (F) Naïve $CD4^{+}$ $CD25^{-}$ T cells from HD were co-cultured with Pso or HD monocytes upon LPS stimulation or without it as indicated. Percentage of IL-17A –expressing $CD4^{+}$ T cell (gated on Live $Lin^{-}$ $CD4^{+}$ cells) in trans well co-culture of monocytes-T cells quantified by flow cytometry (n = 3). The gene expression of *IL17A*, *IL17F*, and *RORC* were quantified by qPCR from HD T cells in co-culture of LPS-stimulated Pso monocytes or HD monocyte. The production of TGF-β1, IL-6, and IL-23 cytokines were quantified by ELISA, from supernatant of T cells in co-culture of LPS-stimulated Pso monocytes or HD monocyte (n = 5). (Error bars show means ± SEM, P values were calculated using Wilcoxon signed rank test).

48 h. Flow cytometry analysis revealed that LPS-stimulated Pso monocytes induced IL-17A production in HD $CD4^{+}$ T cells compared to unstimulated ones and HD monocytes (Fig. 3F). Subsequently, we evaluated the levels of IL-6, IL-23, and TGF-β1 cytokines in the supernatant of the lower well in our co-culture system. As shown in Fig. 3F and Fig. S3B, IL-6, IL-23, and TGF-β1 production, as well as *IL17A*, *IL17F*, and *RORC* (Th17 gene signature) gene expression, were upregulated in both LPS-stimulated and unstimulated Pso monocytes co-cultures compared to HD monocytes. This data reveals that Pso monocytes induce the differentiation of naïve $CD4^{+}$ cells into Th17 cells.

### 3.4. KDM6A/B inhibition reverses trained immunity in Pso monocytes and LL37/self-DNA complex-treated HD monocytes

Recent studies have revealed the upregulation of KDM6A/B in monocytes derived from patients with SLE [27]. A KDM6A/B inhibitor effectively blocked excessive TNF-α production [31] and reduced interferon-stimulated genes (ISG) expression in monocytes from SLE patients [27]. Given the augmented expression of KDM6A/B in Pso monocytes (Fig. 2B) and following 24-h stimulation with LL37/self-DNA complexes in HD monocytes (Fig. 1A), we investigated whether inhibiting KDM6A/B could reverse the enhanced immune responses. Utilizing GSK-J4, a selective inhibitor of KDM6A/B [36], we examined its impact on monocytes. Preincubation of HD monocytes with GSK-J4 (2 μM, nontoxic dose [27,31]) for one hour before 24 h stimulation with LL37/self-DNA complex reduced the activity of KDM6A/B in HD monocytes to the baseline level (unstimulated HD monocytes) and increased the histone repressive H3K27me3 marks compared to LL37/self-DNA-trained and untreated HD monocytes (Fig. 4A and Fig. S4).

GSK-J4 significantly reduced the release of key proinflammatory cytokines including IL-8 and IL-6, after 24 h of LL37/self-DNA complex stimulation (Fig. 4B) and IL-8 and TNF-α during the resting phase in HD monocytes (Fig. 4C). Chromatin immunoprecipitation PCR showed GSK-J4 treatment significantly enriched the deposition of the H3K27me3 mark at the promoter regions of the *IL6* and *TNF* genes after stimulation of HD monocytes treated with LL37/self-DNA complexes within 24 h (Fig. 4D). These findings emphasize the pivotal role of KDM6A/B modifiers in facilitating the heightened cytokine production in LL37/self-DNA-treated HD monocytes. GSK-J4 suppressed the LL37/self-DNA-induced activation of non-histone targets such as NF-κB and STAT3 pathway signaling in treated HD monocytes (Fig. 4E and Fig. S4). Likewise, flow cytometric and western blot analyses showed that GSK-J4 diminished the activated NF-κB and STAT3 in Pso monocytes (Fig. 4F).

Subsequently, we examined whether inhibiting KDM6A/B using GSK-J4 could reverse the metabolic reprogramming observed in LL37/self-DNA-treated HD monocytes. The epigenetic enzyme inhibitor robustly reverted the glycolytic and OXPHOS activities of HD monocytes treated with LL37/self-DNA (Fig. 4G) to lower than baseline levels. Remarkably, GSK-J4 effectively reduced the heightened cytokine responses observed in Pso monocytes upon TLR4 and TLR7/8 stimulations for 24 h and reverted the glycolytic and OXPHOS activities of Pso monocytes (Fig. 4H).

These results underline the profound influence of KDM6A/B inhibition in not only abating the exaggerated cytokine responses elicited by LL37/self-DNA complexes but also in reversing the aberrant metabolic and epigenetic reprogramming observed in psoriatic monocytes, thereby highlighting the therapeutic potential of targeting KDM6A/B [36] in modulating inflammatory responses and metabolic dysregulation.

### 3.5. The effect of LL37/self-DNA-treated HD monocytes on naive HD $CD4^{+}$ T cells

As shown previously, soluble mediators released by psoriatic (Pso) monocytes induce the differentiation of naive $CD4^{+}$ cells into Th17 cells, characterized by higher expression of *IL17A*, *IL17F*, and *RORC*, and the secretion of IL-6, IL-23, and TGF-β1 cytokines (Fig. 3F). This raises the question of whether secreted mediators from LL37/self-DNA-treated HD monocytes affect cytokine production and differentiation of naive HD $CD4^{+}$ T cells. To investigate this, HD monocytes were subjected to LL37/self-DNA stimulation within trans-well plate inserts and co-cultured with naive $CD4^{+}$ T cells at a 25:75 T cells/monocytes ratio (Fig. S3A) [23,24]. After 24 h of culture, the top inserts containing LL37/self-DNA-treated HD monocytes were removed, and the T cells were analyzed after 48 h. Flow cytometry analysis revealed that LL37/self-DNA-treated HD monocytes induced the IL-17A production in $CD4^{+}$ T cells compared to unstimulated HD monocytes (11.9% *versus* 1.8%). Notably, the IL-17A production was significantly inhibited in the LL37/self-DNA-GSK-J4 treated group (11.9% *versus* 3.8%). The culture of naïve T cells alone (in the absence of monocytes) with LL37/self-DNA complexes did not affect IL-17A production in $CD4^{+}$ T cells (Fig. 5A).

Subsequently, we evaluated the local cytokine milieu in our co-culture system's supernatant of T cells. After 24 h of culture, the top inserts containing LL37/self-DNA-treated HD monocytes were removed, and the supernatant from the lower well was analyzed with the Proteome Profiler Human XL Cytokine Array after 48 h. Following image analysis and the quantification of pixel intensity for each spot, 105 cytokines were evaluated in the supernatant of LL37/self-DNA-treated HD compared to unstimulated HD monocytes-T cells co-culture (Fig. 5B). Of these, 17 cytokines were upregulated after LL37/self-DNA treatment in co-culture, including molecules known to play roles in pathogenic response cytokines (IL-6, IL-1β, GM-CSF, and IL-17A) [37] were also strongly downregulated after LL37/DNA-GSK-J4 treatment (except IL-8). The names of these differentially expressed 5 cytokines/chemokines are presented on a schematic grid that corresponds to the spot positions on the membrane. In keeping with the literature [38], we detected that most inflammatory cytokines, specifically IL-6, were inhibited after LL37/DNA-GSK-J4 treatment, indicating a return to baseline levels similar to the unstimulated group (Fig. 4B). Furthermore, IL-6 and TGF-β1 production was upregulated after LL37/self-DNA treatment in co-culture and were strongly downregulated after LL37/DNA-GSK-J4 treatment (Fig. 5D). Notably, the expression of *IL17A*, *IL17F*, and *RORC* was not changed in T cells in both culture systems, and IL-23 cytokine was not secreted in their supernatants. This data reveals that LL37/self-DNA-treated HD monocytes, unlike LL37 alone (Fig. S5), induce the naïve $CD4^{+}$ cells into IL-17-producing cells, but not into Th17

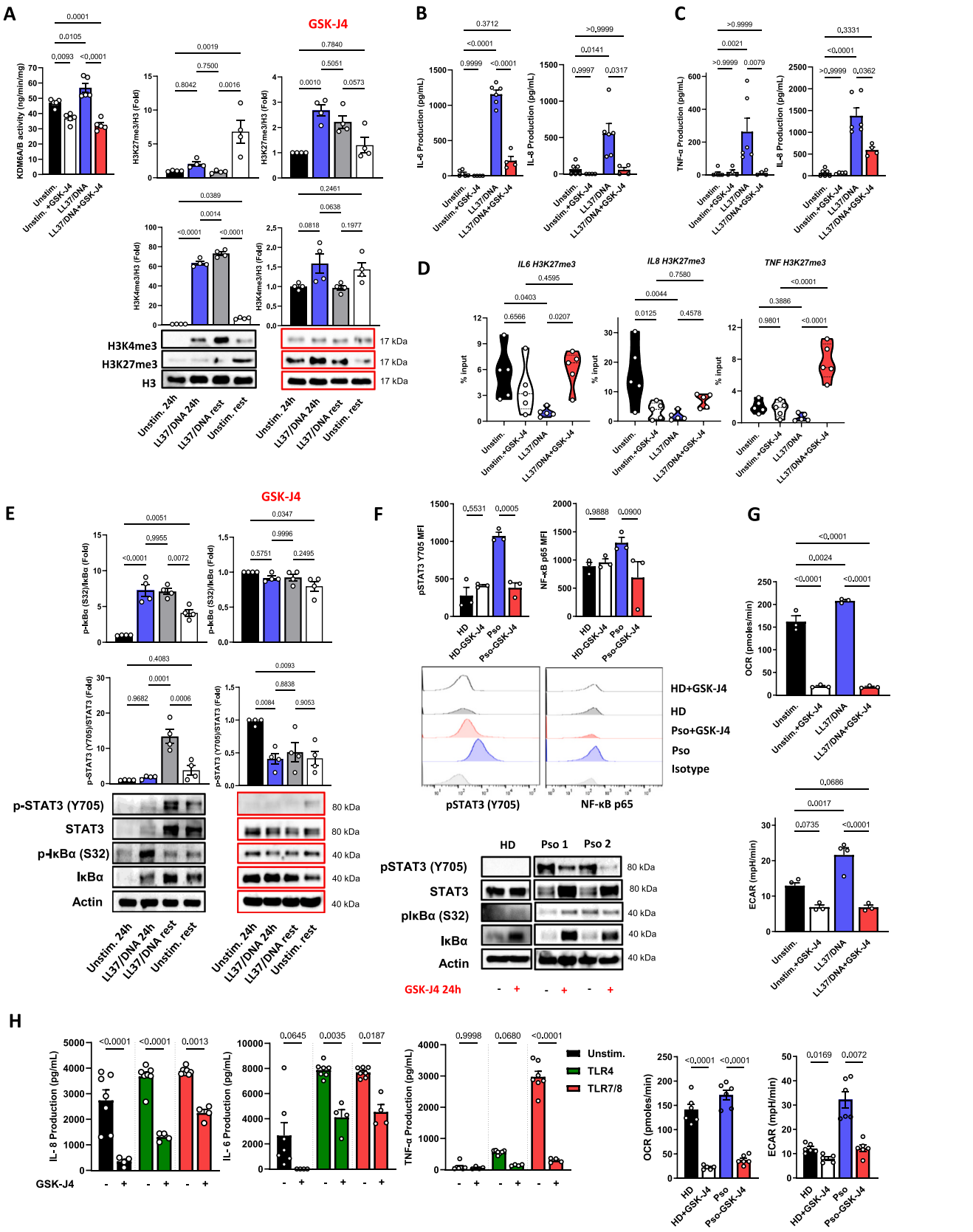


*(caption on next page)*

**Fig. 4.** Impact of KDM6A/B inhibition on LL37/self-DNA-treated HD monocytes and Pso monocytes. (A) Treatment with GSK-J4 normalized the heightened activity of KDM6A/B in LL37/self-DNA-treated HD monocytes, reducing it to baseline levels (n = 5) and increasing H3K27me3 marks. (B) Preincubation of HD monocytes with GSK-J4, one hour before LL37/self-DNA complex stimulation for 24 h, significantly decreased the release of IL-8 and IL-6 at 24 h post-stimulation (n = 4). (C) GSK-J4 treatment reduced IL-8, IL-6, and TNF-α levels during the resting phase following LL37/self-DNA complex stimulation, demonstrating a sustained effect on cytokine reduction (n = 4). (D) GSK-J4 effectively increased H3K27me3 marks at the promoter regions of *IL6 and TNF* (but not *IL8*) genes following LL37/self-DNA complex stimulation (n = 5). (E) Western blot analysis depicting p-STAT3, STAT3, p-IκB, and IκB in HD monocytes treated with GSK-J4 one hour before LL37/self-DNA complex stimulation. (F) Flow cytometry and western blot analysis depicting reduced STAT3 and NF-κB activation in Pso monocytes treated with GSK-J4 compared to HD monocytes (n = 3). (G) GSK-J4 intervention reversed the enhanced glycolytic and oxidative phosphorylation activities observed in LL37/self-DNA-trained HD monocytes (n = 3). (H) GSK-J4 effectively mitigated the exaggerated cytokine responses observed in Pso monocytes upon TLR4 and TLR7/8 stimulation (n = 4–7) and the enhanced glycolytic and oxidative phosphorylation activities (n = 6). (Error bars show means ± SEM, P values were calculated using Wilcoxon signed rank test).

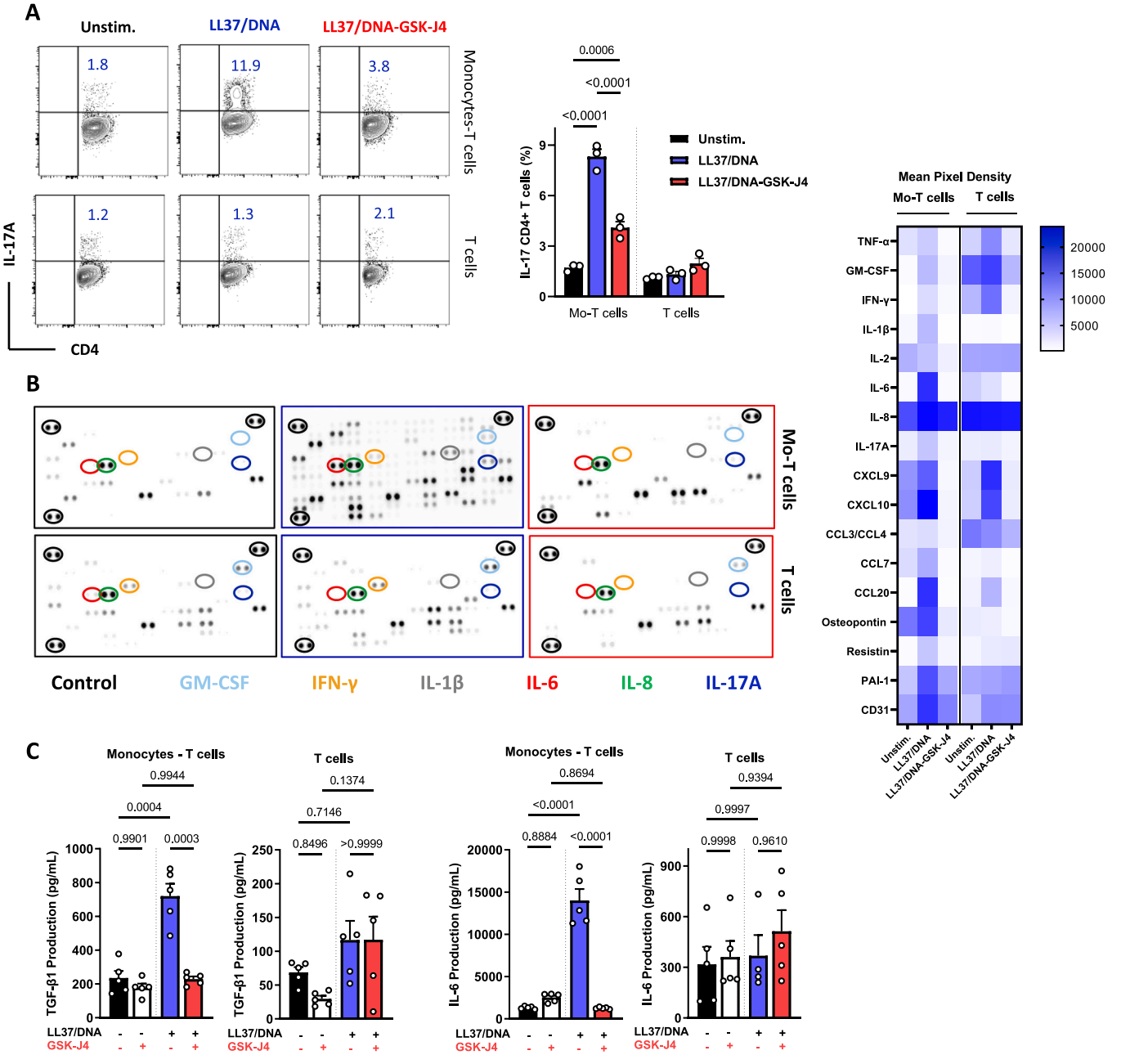


**Fig. 5.** Impact of LL37/self-DNA-treated HD monocytes and their KDM6A/B inhibition on naive HD $CD4^+$ T cells. (A) Naive $CD4^+$ $CD25^-$ T cells and LL37/self-DNA-treated HD monocytes were co-cultured as indicated. The percentage of IL-17A–expressing $CD4^+$ T cells (gated on Live $Lin^-$ $CD4^+$ cells) in the transwell co-culture of monocytes-T cells and T cell culture alone was quantified by flow cytometry (n = 3). (B) After 24 h of culture, LL37/self-DNA-treated HD monocytes were removed, and the supernatant from the lower well of the co-culture was analyzed after 48 h using a Proteome Profiler Human XL Cytokine Array (n = 4). (C) The production of IL-6 and TGF-β1 was quantified by ELISA in cell supernatants from the transwell co-culture of monocytes-T cells and T cell culture alone (n = 5). (Error bars show means ± SEM, P values were calculated using one-way ANOVA followed by Dunnett's multiple comparisons test.).

cells. Additionally, HD monocytes exert a synergistic increase effect by upregulating the secretion of GM-CSF, IL-1β, IL-6, TGF-β1, and IL-17A upon LL37/self-DNA exposure in trans-well co-culture.

## 4. Discussion

Recent findings support the concept that alterations in metabolism also affect the epigenetics of monocytes, contributing to the concept of innate immune memory [1,4]. In this study, we demonstrated that LL37/self-DNA complexes, to a lesser extent LL37, induce monocyte reprogramming at metabolic and epigenetic levels, enhancing responsiveness to subsequent stimuli. Our observations revealed heightened glycolysis and oxidative phosphorylation rates in LL37/self-DNA-trained monocytes as well as in peripheral monocytes from psoriasis patients. These metabolic shifts indicate a heightened readiness to respond to inflammatory stimuli, by increased releases of proinflammatory cytokines, including IL-6, IL-8, and TNF-α, and elevated ROS production. The link between metabolic reprogramming and trained immunity is further supported by our observation that inhibiting glycolysis with 2-deoxy-D-glucose (2-DG) reduced STAT3 and NF-κB activation in LL37/self-DNA-treated monocytes.

Epigenetic modifications regulate transcription and contribute to trained immunity responsiveness [39]. Here, we observed the enrichment of activating H3K4me3 marks and the reduction in repressive H3K27me3 marks on the promoter regions of proinflammatory cytokine genes, *TNF* and *IL6* in LL37/self-DNA-trained monocytes This epigenetic remodeling primes monocytes for enhanced responsiveness to subsequent stimuli. Given the differential expression levels of H3K27me3 in global and promoter regions of *TNF* and *IL6*, it suggests additional aspects of epigenomic regulation. Future studies should aim to elucidate further the genome-wide epigenetic changes induced by LL37/self-DNA complexes, focusing on identifying which regions are silenced or activated. Understanding these dynamics could provide deeper insights into the mechanisms of trained immunity and aid in the developing more targeted therapeutic strategies.

It was recently shown that the accumulation of α-ketoglutarate (α-KG) as a cofactor of KDM6A/B integrates metabolic circuits to induce monocyte epigenetic reprogramming [27,40]. Additionally, using Gas chromatography (GC) TOF-MS, revealed that psoriasis patients had higher levels of α-ketoglutarate (α-KG) in their serum compared to healthy individuals [41]. Consistent with the peripheral blood of RA and SLE patients, where LL37/self-DNA plays a significant role in the pathogenesis of these diseases, we found that the KDM6B enzyme was upregulated in isolated monocytes from psoriatic patients compared to healthy controls [27,42].

The upregulation of KDM6A/B enzyme activity in response to LL37/self-DNA complexes indicated potential epigenetic alterations akin to those observed in psoriatic monocytes. This upregulation contributed to enhanced demethylation and removal of repressive H3K27me3 histone marks [27] allowing for the activation of genes encoding proinflammatory cytokines.

Using GSK-4 J, a KDM6A/B-selective inhibitor [31], we effectively reversed innate immune memory in LL37/self-DNA-trained monocytes and psoriatic monocytes. This inhibition mitigated proinflammatory cytokine production, NF-kB-STAT3 signaling, and metabolic activities. Recent studies have shown that type I IFN induces innate immune memory in SLE monocytes, accompanied by epigenetic changes, including increased H3K4me3 and decreased H3K27me3 at IFN-stimulated genes (ISGs) promoter sites. These findings suggest that KDM6A/B demethylases are highly regulated at the transcriptional level, and their functional activity in trained monocytes may involve various pathways in SLE [27] as we observed in psoriasis. KDM6A/B's role in regulating broad proinflammatory gene expression emphasizes its therapeutic potential in inflammatory conditions [27,30,31,40,42–44]. As shown the inflammatory cytokine milieu induced by psoriatic monocytes contributed to Th17 differentiation and may play a crucial role in disease pathogenesis [45]. LL37/self-DNA-treated monocytes have the capacity to produce higher levels of IL-8, IL-6, and TNF-α and attract to inflammatory cells by a synergistic increase of C—C motif ligand (CCL) 3, CCL4, CCL7, and CCL20. They can further differentiate into inflammatory macrophages or DCs, infiltrate T cell areas, and amplify T cell responses. As shown, LL37/self-DNA-treated HD monocytes induced the differentiation of naive $CD4^+$ T cells into IL-17-producing cells, albeit not fully into Th17 cells. Recent studies showed that KDM6B demethylases and α-KG play a central role in the metabolism, epigenetics, and functional landscape of human and murine $CD4^+$ T cell subsets [38,46]. GSK-J4 dramatically suppresses Th17 cell differentiation *in vitro* and *in vivo* [46]. GSK-J4 was shown to bind to and reduce the levels of H3K27me3 directly, impacting the RORγt transcription factor, and inducing metabolic reprogramming in Th17 cells toward a resting state, leading to the suppression of Th17 differentiation [37,38,46]. Our findings demonstrated that GSK-J4 treatment successfully returned $CD4^+$ T cells and their cytokine milieu to baseline levels. Furthermore, KDM6A/B inhibition restored the epigenetic landscape to a more repressive state, as evidenced by increased H3K27me3 marks on the promoters of IL6 and TNF. Thus, targeting specific mechanisms at the epigenetic level, participating not only in the functional activity of trained monocytes but also in IL-17-producing T cells, might be a beneficial strategy for treatment to reduce the chronicity and severity of psoriasis.

## 5. Conclusions

Our findings highlight the crucial role of LL37/self-DNA complexes in driving both metabolic and epigenetic reprogramming in monocytes, thereby contributing to the pathogenesis of psoriasis and potentially other autoimmune diseases. Understanding prolonged metabolic reprogramming mechanisms remains an area for future inquiry, including whether monocyte reprogramming originates from hematopoietic progenitors in the bone marrow [47,48]. Exploring additional layers of epigenomic regulation that modulate innate immune memory is also crucial [49]. Taken together, our findings provide a basis for further exploration using small molecule KDM6A/B inhibitors to comprehend these critical aspects of innate immune memory. KDM6A/B emerges as a promising therapeutic target for chronic, relapsing, and systemic inflammatory diseases, including psoriasis, supported by studies emphasizing its role in Th17 cell differentiation and innate memory.

## Funding sources

This work was supported by the German Research Foundation (Deutsche Forschungsgemeinschaft-DFG), grants ZA 1247/1-1 (project number 507777753) to F.S. Additional support was received from the CRC1066, TP-B14 to A.T., Wilhelm-Sander-Foundation (2020-132.2) to A.T., Hiege-Stiftung against skin cancer (200504) to A.T., and Peter-Hans Hofschneider Foundation to D.K., the DFG TRR156/3 (project number 246807620) to D.K., and TRR355/1 (project number 490846870) to D.K.

## CRediT authorship contribution statement

**Aman Damara:** Methodology, Formal analysis, Data curation. **Joanna Wegner:** Project administration, Methodology, Data curation. **Emily R. Trzeciak:** Formal analysis, Data curation. **Antonia Kolb:** Formal analysis, Data curation. **Mahsa Nastaranpour:** Data curation. **Rahul Khatri:** Data curation. **Andrea Tuettenberg:** Writing – review & editing, Funding acquisition. **Daniela Kramer:** Writing – review & editing, Funding acquisition. **Stephan Grabbe:** Writing – review & editing, Resources, Project administration. **Fatemeh Shahneh:** Writing – review & editing, Writing – original draft, Validation, Supervision, Investigation, Funding acquisition, Formal analysis, Conceptualization.

## Declaration of competing interest

The authors declare that they have no known competing financial interests or personal relationships that could have appeared to influence the work reported in this paper.

## Data availability

All data relevant to the study are included in the article or uploaded as supplementary information.

## Acknowledgement

We thank our patients for their participation in our studies.

## Appendix A. Supplementary data

Supplementary data to this article can be found online at https://doi.org/10.1016/j.clim.2024.110287.

## References

[1] M.G. Netea, J. Domínguez-Andrés, L.B. Barreiro, T. Chavakis, M. Divangahi, E. Fuchs, L.A.B. Joosten, J.W.M. van der Meer, M.M. Mhlanga, W.J.M. Mulder, N. P. Riksen, A. Schlitzer, J.L. Schultze, C. Stabell Benn, J.C. Sun, R.J. Xavier, E. Latz, Defining trained immunity and its role in health and disease, Nat. Rev. Immunol. 20 (2020) 375–388, https://doi.org/10.1038/s41577-020-0285-6.

[2] S. Bekkering, R.J.W. Arts, B. Novakovic, I. Kourtzelis, C.D.C.C. van der Heijden, Y. Li, C.D. Popa, R. ter Horst, J. van Tuijl, R.T. Netea-Maier, F.L. van de Veerdonk, T. Chavakis, L.A.B. Joosten, J.W.M. van der Meer, H. Stunnenberg, N.P. Riksen, M. G. Netea, Metabolic induction of trained immunity through the mevalonate pathway, Cell 172 (2018) 135–146.e9, https://doi.org/10.1016/j.cell.2017.11.025.

[3] A.V. Ferreira, S. Kostidis, L.A. Groh, V.A.C.M. Koeken, M. Bruno, I. Baydemir, G. Kilic, Ö. Bulut, T. Andriopoulou, V. Spanou, K.D. Synodinou, T. Gkavogianni, S. J.C.F.M. Moorlag, L. Charlotte de Bree, V.P. Mourits, V. Matzaraki, W.J. H. Koopman, F.L. van de Veerdonk, G. Renieris, M. Giera, E.J. Giamarellos-Bourboulis, B. Novakovic, J. Domínguez-Andrés, Dimethyl itaconate induces long-term innate immune responses and confers protection against infection, Cell Rep. 42 (2023), https://doi.org/10.1016/j.celrep.2023.112658.

[4] S. Fanucchi, J. Domínguez-Andrés, L.A.B. Joosten, M.G. Netea, M.M. Mhlanga, The intersection of epigenetics and metabolism in trained immunity, Immunity 54 (2021) 32–43, https://doi.org/10.1016/j.immuni.2020.10.011.

[5] R.M. Rodriguez, B. Suarez-Alvarez, C. Lopez-Larrea, Therapeutic epigenetic reprogramming of trained immunity in myeloid cells, Trends Immunol. 40 (2019) 66–80, https://doi.org/10.1016/j.it.2018.11.006.

[6] S. Bekkering, J. Domínguez-Andrés, L.A.B. Joosten, N.P. Riksen, M.G. Netea, Trained Immunity: Reprogramming Innate Immunity in Health and Disease Keywords, 2021, https://doi.org/10.1146/annurev-immunol-102119.

[7] S.-C. Cheng, J. Quintin, R.A. Cramer, K.M. Shepardson, S. Saeed, V. Kumar, E. J. Giamarellos-Bourboulis, J.H.A. Martens, N.A. Rao, A. Aghajanirefah, G. R. Manjeri, Y. Li, D.C. Ifrim, R.J.W. Arts, B.M.J.W. Van Der Veer, P.M.T. Deen, C. Logie, L.A. O'neill, P. Willems, F.L. Van De Veerdonk, J.W.M. Van Der Meer, A. Ng, L.A.B. Joosten, C. Wijmenga, H.G. Stunnenberg, R.J. Xavier, M.G. Netea, mTOR-and HIF-1a-Mediated Aerobic Glycolysis as Metabolic basis for Trained Immunity. https://www.science.org, 2024.

[8] J. Ochando, W.J.M. Mulder, J.C. Madsen, M.G. Netea, R. Duivenvoorden, Trained immunity — basic concepts and contributions to immunopathology, Nat. Rev. Nephrol. 19 (2023) 23–37, https://doi.org/10.1038/s41581-022-00633-5.

[9] F. Herster, Z. Bittner, N.K. Archer, S. Dickhöfer, D. Eisel, T. Eigenbrod, T. Knorpp, N. Schneiderhan-Marra, M.W. Löffler, H. Kalbacher, T. Vierbuchen, H. Heine, L. S. Miller, D. Hartl, L. Freund, K. Schäkel, M. Heister, K. Ghoreschi, A.N.R. Weber, Neutrophil extracellular trap-associated RNA and LL37 enable self-amplifying inflammation in psoriasis, Nat. Commun. 11 (2020), https://doi.org/10.1038/s41467-019-13756-4.

[10] L.B. Olson, N.I. Hunter, R.E. Rempel, B.A. Sullenger, Targeting DAMPs with nucleic acid scavengers to treat lupus, Transl. Res. 245 (2022) 30–40, https://doi.org/10.1016/j.trsl.2022.02.007.

[11] D. Badal, D. Dayal, G. Singh, N. Sachdeva, Role of DNA-LL37 complexes in the activation of plasmacytoid dendritic cells and monocytes in subjects with type 1 diabetes, Sci. Rep. 10 (2020), https://doi.org/10.1038/s41598-020-65851-y.

[12] N. Kang, X. Liu, K. Haneef, W. Liu, Old and new damage-associated molecular patterns (DAMPs) in autoimmune diseases, Rheumatol. Autoimmunity 2 (2022) 185–197, https://doi.org/10.1002/rai2.12046.

[13] R.M. van Harten, E. van Woudenbergh, A. van Dijk, H.P. Haagsman, Cathelicidins: immunomodulatory antimicrobials, Vaccines (Basel) 6 (2018), https://doi.org/10.3390/vaccines6030063.

[14] R. Lande, J. Gregorio, V. Facchinetti, B. Chatterjee, Y.H. Wang, B. Homey, W. Cao, Y.H. Wang, B. Su, F.O. Nestle, T. Zal, I. Mellman, J.M. Schröder, Y.J. Liu, M. Gilliet, Plasmacytoid dendritic cells sense self-DNA coupled with antimicrobial peptide, Nature 449 (2007) 564–569, https://doi.org/10.1038/nature06116.

[15] L. Frasca, R. Palazzo, M.S. Chimenti, S. Alivernini, B. Tolusso, L. Bui, E. Botti, A. Giunta, L. Bianchi, L. Petricca, S.E. Auteri, F. Spadaro, G.L. Fonti, M. Falchi, A. Evangelista, B. Marinari, I. Pietraforte, F.R. Spinelli, T. Colasanti, C. Alessandri, F. Conti, E. Gremese, A. Costanzo, G. Valesini, R. Perricone, R. Lande, Anti-LL37 antibodies are present in psoriatic arthritis (PsA) patients: new biomarkers in PsA, Front. Immunol. 9 (2018), https://doi.org/10.3389/fimmu.2018.01936.

[16] B.B. Sen, E.N. Rifaioglu, O. Ekiz, M.U. Inan, T. Sen, N. Sen, Neutrophil to lymphocyte ratio as a measure of systemic inflammation in psoriasis, Cutan. Ocul. Toxicol. 33 (2014) 223–227, https://doi.org/10.3109/15569527.2013.834498.

[17] D. Ganguly, G. Chamilos, R. Lande, J. Gregorio, S. Meller, V. Facchinetti, B. Homey, F.J. Barrat, T. Zal, M. Gilliet, Self-RNA-antimicrobial peptide complexes activate human dendritic cells through TLR7 and TLR8, J. Exp. Med. 206 (2009) 1983–1994, https://doi.org/10.1084/jem.20090480.

[18] G. Chamilos, J. Gregorio, S. Meller, R. Lande, D.P. Kontoyiannis, R.L. Modlin, M. Gilliet, Cytosolic sensing of extracellular self-DNA transported into monocytes by the antimicrobial peptide LL37, Blood 120 (2012) 3699–3707, https://doi.org/10.1182/blood-2012-01-401364.

[19] J.B. Golden, S.G. Groft, M.V. Squeri, S.M. Debanne, N.L. Ward, T.S. McCormick, K. D. Cooper, Chronic psoriatic skin inflammation leads to increased monocyte adhesion and aggregation, J. Immunol. 195 (2015) 2006–2018, https://doi.org/10.4049/jimmunol.1402307.

[20] T.S. Kapellos, L. Bonaguro, I. Gemünd, N. Reusch, A. Saglam, E.R. Hinkley, J. L. Schultze, Human monocyte subsets and phenotypes in major chronic inflammatory diseases, Front. Immunol. 10 (2019), https://doi.org/10.3389/fimmu.2019.02035.

[21] M.C. Costa, C.S. Paixão, D.L. Viana, B. de O. Rocha, M. Saldanha, L.M.H. da Mota, P.R.L. Machado, C. Pagliari, M. De F. de Oliveira, S. Arruda, E.M. Carvalho, L. P. Carvalho, Mononuclear phagocyte activation is associated with the immunopathology of psoriasis, Front. Immunol. 11 (2020), https://doi.org/10.3389/fimmu.2020.00478.

[22] J. Domínguez-Andrés, R.J.W. Arts, S. Bekkering, H. Bahrar, B.A. Blok, L.C.J. de Bree, M. Bruno, Ö. Bulut, P.A. Debisarun, H. Dijkstra, J. Cristina dos Santos, A. V. Ferreira, D. Flores-Gomez, L.A. Groh, I. Grondman, L. Helder, C. Jacobs, L. Jacobs, T. Jansen, G. Kilic, V. Klück, V.A.C.M. Koeken, H. Lemmers, S.J.C.F. M. Moorlag, V.P. Mourits, J.H. van Puffelen, K. Rabold, R.J. Röring, D. Rosati, H. Tercan, J. van Tuijl, J. Quintin, R. van Crevel, N.P. Riksen, L.A.B. Joosten, M. G. Netea, In vitro induction of trained immunity in adherent human monocytes, STAR Protoc 2 (2021), https://doi.org/10.1016/j.xpro.2021.100365.

[23] C.A. Roberts, A.K. Dickinson, L.S. Taams, The interplay between monocytes/macrophages and CD4+ T cell subsets in rheumatoid arthritis, Front. Immunol. 6 (2015), https://doi.org/10.3389/fimmu.2015.00571.

[24] S.B. Schrier, A.S. Hill, D. Plana, D.A. Lauffenburger, Synergistic communication between CD4+ T cells and monocytes impacts the cytokine environment, Sci. Rep. 6 (2016), https://doi.org/10.1038/srep34942.

[25] R.J.W. Arts, B. Novakovic, R. ter Horst, A. Carvalho, S. Bekkering, E. Lachmandas, F. Rodrigues, R. Silvestre, S.C. Cheng, S.Y. Wang, E. Habibi, L.G. Gonçalves, I. Mesquita, C. Cunha, A. van Laarhoven, F.L. van de Veerdonk, D.L. Williams, J.W. M. van der Meer, C. Logie, L.A. O'Neill, C.A. Dinarello, N.P. Riksen, R. van Crevel, C. Clish, R.A. Notebaart, L.A.B. Joosten, H.G. Stunnenberg, R.J. Xavier, M.G. Netea, Glutaminolysis and fumarate accumulation integrate Immunometabolic and epigenetic programs in trained immunity, Cell Metab. 24 (2016) 807–819, https://doi.org/10.1016/j.cmet.2016.10.008.

[26] S.T. Keating, L. Groh, K. Thiem, S. Bekkering, Y. Li, V. Matzaraki, C.D.C.C. van der Heijden, J.H. van Puffelen, E. Lachmandas, T. Jansen, M. Oosting, L.C.J. de Bree, V. A.C.M. Koeken, S.J.C.F.M. Moorlag, V.P. Mourits, J. van Diepen, R. Strienstra, B. Novakovic, H.G. Stunnenberg, R. van Crevel, L.A.B. Joosten, M.G. Netea, N. P. Riksen, Rewiring of glucose metabolism defines trained immunity induced by oxidized low-density lipoprotein, J. Mol. Med. 98 (2020) 819–831, https://doi.org/10.1007/s00109-020-01915-w.

[27] E.N. Montano, M. Bose, L. Huo, G. Tumurkhuu, G. De Los Santos, B. Simental, A. B. Stotland, J. Wei, C.N. Bairey Merz, J. Suda, G. Martins, S. Lalani, K. Lawrenson, Y. Wang, S. Parker, S. Venuturupalli, M. Ishimori, D.J. Wallace, C.A. Jefferies, α-ketoglutarate-dependent KDM6 histone demethylases regulate interferon stimulated gene expression in lupus, Arthritis Rheum. (2023), https://doi.org/10.1002/art.42724.

[28] D. Capece, D. Verzella, I. Flati, P. Arboretto, J. Cornice, G. Franzoso, NF-κB: blending metabolism, immunity, and inflammation, Trends Immunol. 43 (2022) 757–775, https://doi.org/10.1016/j.it.2022.07.004.

[29] F. De Santa, M.G. Totaro, E. Prosperini, S. Notarbartolo, G. Testa, G. Natoli, The histone H3 Lysine-27 demethylase Jmjd3 links inflammation to inhibition of polycomb-mediated gene silencing, Cell 130 (2007) 1083–1094, https://doi.org/10.1016/j.cell.2007.08.019.

[30] S. Ma, L. Xu, L. Chen, X. Sun, F. Hu, Y. Gong, R. Yang, J. Li, Q. Wang, S. Huang, H. Zhou, J. Wang, Novel pharmacological inhibition of JMJD3 improves necrotizing enterocolitis by attenuating the inflammatory response and ameliorating intestinal injury, Biochem. Pharmacol. 203 (2022), https://doi.org/10.1016/j.bcp.2022.115165.

[31] L. Kruidenier, C.W. Chung, Z. Cheng, J. Liddle, K. Che, G. Joberty, M. Bantscheff, C. Bountra, A. Bridges, H. Diallo, D. Eberhard, S. Hutchinson, E. Jones, R. Katso, M. Leveridge, P.K. Mander, J. Mosley, C. Ramirez-Molina, P. Rowland, C. J. Schofield, R.J. Sheppard, J.E. Smith, C. Swales, R. Tanner, P. Thomas, A. Tumber, G. Drewes, U. Oppermann, D.J. Patel, K. Lee, D.M. Wilson, A selective jumonji H3K27 demethylase inhibitor modulates the proinflammatory macrophage response, Nature 488 (2012) 404–408, https://doi.org/10.1038/nature11262.

[32] N.D. Das, K.H. Jung, M.R. Choi, H.S. Yoon, S.H. Kim, Y.G. Chai, Gene networking and inflammatory pathway analysis in a JMJD3 knockdown human monocytic cell line, Cell Biochem. Funct. 30 (2012) 224–232, https://doi.org/10.1002/cbf.1839.
[33] M.M. Sherry-Lynes, S. Sengupta, S. Kulkarni, B.H. Cochran, Regulation of the JMJD3 (KDM6B) histone demethylase in glioblastoma stem cells by STAT3, PLoS One 12 (2017), https://doi.org/10.1371/journal.pone.0174775.
[34] G.D. Thomas, A.A.J. Hamers, C. Nakao, P. Marcovecchio, A.M. Taylor, C. McSkimming, A.T. Nguyen, C.A. McNamara, C.C. Hedrick, Human blood monocyte subsets: a new gating strategy Defned using cell surface markers identifed by mass cytometry, Arterioscler. Thromb. Vasc. Biol. 37 (2017) 1548–1558, https://doi.org/10.1161/ATVBAHA.117.309145.
[35] M. Jagannathan-Bogdan, M.E. McDonnell, H. Shin, Q. Rehman, H. Hasturk, C. M. Apovian, B.S. Nikolajczyk, Elevated proinflammatory cytokine production by a skewed T cell compartment requires monocytes and promotes inflammation in type 2 diabetes, J. Immunol. 186 (2011) 1162–1172, https://doi.org/10.4049/jimmunol.1002615.
[36] J. Abu-Hanna, J.A. Patel, E. Anastasakis, R. Cohen, L.H. Clapp, M. Loizidou, M.M. R. Eddama, Therapeutic potential of inhibiting histone 3 lysine 27 demethylases: a review of the literature, Clin. Epigenetics 14 (2022), https://doi.org/10.1186/s13148-022-01305-8.
[37] A. Wagner, C. Wang, J. Fessler, D. DeTomaso, J. Avila-Pacheco, J. Kaminski, S. Zaghouani, E. Christian, P. Thakore, B. Schellhaass, E. Akama-Garren, K. Pierce, V. Singh, N. Ron-Harel, V.P. Douglas, L. Bod, A. Schnell, D. Puleston, R.A. Sobel, M. Haigis, E.L. Pearce, M. Soleimani, C. Clish, A. Regev, V.K. Kuchroo, N. Yosef, Metabolic modeling of single Th17 cells reveals regulators of autoimmunity, Cell 184 (2021) 4168–4185.e21, https://doi.org/10.1016/j.cell.2021.05.045.
[38] A.P. Cribbs, S. Terlecki-Zaniewicz, M. Philpott, J. Baardman, D. Ahern, M. Lindow, S. Obad, H. Oerum, B. Sampey, P.K. Mander, H. Penn, P. Wordsworth, P. Bowness, M. de Winther, R.K. Prinjha, M. Feldmann, U. Oppermann, Histone H3K27me3 demethylases regulate human Th17 cell development and effector functions by impacting on metabolism, Proc. Natl. Acad. Sci. 117 (2020) 6056–6066, https://doi.org/10.1073/pnas.1919893117.
[39] M. Divangahi, P. Aaby, S.A. Khader, L.B. Barreiro, S. Bekkering, T. Chavakis, R. van Crevel, N. Curtis, A.R. DiNardo, J. Dominguez-Andres, R. Duivenwoorden, S. Fanucchi, Z. Fayad, E. Fuchs, M. Hamon, K.L. Jeffrey, N. Khan, L.A.B. Joosten, E. Kaufmann, E. Latz, G. Matarese, J.W.M. van der Meer, M. Mhlanga, S.J.C.F. M. Moorlag, W.J.M. Mulder, S. Naik, B. Novakovic, L. O'Neill, J. Ochando, K. Ozato, N.P. Riksen, R. Sauerwein, E.R. Sherwood, A. Schlitzer, J.L. Schultze, M. H. Sieweke, C.S. Benn, H. Stunnenberg, J. Sun, F.L. van de Veerdonk, S. Weis, D. L. Williams, R. Xavier, M.G. Netea, Trained immunity, tolerance, priming and differentiation: distinct immunological processes, Nat. Immunol. 22 (2021) 2–6.
[40] K. Ming-Chin Lee, A.A. Achuthan, D.P. De Souza, T.J. Lupancu, K.J. Binger, M.K. S. Lee, Y. Xu, M.J. McConville, N.A. de Weerd, D. Dragoljevic, P.J. Hertzog, A. J. Murphy, J.A. Hamilton, A.J. Fleetwood, Type I interferon antagonism of the JMJD3-IRF4 pathway modulates macrophage activation and polarization, Cell Rep. 39 (2022), https://doi.org/10.1016/j.celrep.2022.110719.
[41] A.W. Armstrong, J. Wu, M.A. Johnson, D. Grapov, B. Azizi, J. Dhillon, O. Fiehn, Metabolomics in psoriatic disease: Pilot study reveals metabolite differences in psoriasis and psoriatic arthritis, F1000Res 3 (2014).
[42] W. Jia, W. Wu, D. Yang, C. Xiao, Z. Su, Z. Huang, Z. Li, M. Qin, M. Huang, S. Liu, F. Long, J. Mao, X. Liu, Y.Z. Zhu, Histone demethylase JMJD3 regulates fibroblast-like synoviocyte-mediated proliferation and joint destruction in rheumatoid arthritis, FASEB J. 32 (2018) 4031–4042, https://doi.org/10.1096/fj.201701483R.
[43] C. Doñas, J. Neira, F. Osorio-Barrios, M. Carrasco, D. Fernández, C. Prado, A. Loyola, R. Pacheco, M. Rosemblatt, The demethylase inhibitor GSK-J4 limits inflammatory colitis by promoting de novo synthesis of retinoic acid in dendritic cells, Sci. Rep. 11 (2021), https://doi.org/10.1038/s41598-020-79122-3.
[44] M.I. Matias, C.S. Yong, A. Foroushani, C. Goldsmith, C. Mongellaz, E. Sezgin, K. R. Levental, A. Talebi, J. Perrault, A. Rivière, J. Dehairs, O. Delos, J. Bertand-Michel, J.C. Portais, M. Wong, J.C. Marie, A. Kelekar, S. Kinet, V.S. Zimmermann, I. Levental, L. Yvan-Charvet, J.V. Swinnen, S.A. Muljo, H. Hernandez-Vargas, S. Tardito, N. Taylor, V. Dardalhon, Regulatory T cell differentiation is controlled by αKG-induced alterations in mitochondrial metabolism and lipid homeostasis, Cell Rep. 37 (2021), https://doi.org/10.1016/j.celrep.2021.109911.
[45] S. Kagami, H.L. Rizzo, J.J. Lee, Y. Koguchi, A. Blauvelt, Circulating Th17, Th22, and Th1 cells are increased in psoriasis, J. Invest. Dermatol. 130 (2010) 1373–1383, https://doi.org/10.1038/jid.2009.399.
[46] Z. Liu, W. Cao, L. Xu, X. Chen, Y. Zhan, Q. Yang, S. Liu, P. Chen, Y. Jiang, X. Sun, Y. Tao, Y. Hu, C. Li, Q. Wang, Y. Wang, C.D. Chen, Y. Shi, X. Zhang, The histone H3 lysine-27 demethylase Jmjd3 plays a critical role in specific regulation of Th17 cell differentiation, J. Mol. Cell Biol. 7 (2015) 505–516, https://doi.org/10.1093/jmcb/mjv022.
[47] I. Mitroulis, K. Ruppova, B. Wang, L.S. Chen, M. Grzybek, T. Grinenko, A. Eugster, M. Troullinaki, A. Palladini, I. Kourtzelis, A. Chatzigeorgiou, A. Schlitzer, M. Beyer, L.A.B. Joosten, B. Isermann, M. Lesche, A. Petzold, K. Simons, I. Henry, A. Dahl, J. L. Schultze, B. Wielockx, N. Zamboni, P. Mirtschink, Ü. Coskun, G. Hajishengallis, M.G. Netea, T. Chavakis, Modulation of myelopoiesis progenitors is an integral component of trained immunity, Cell 172 (2018) 147–161.e12, https://doi.org/10.1016/j.cell.2017.11.034.
[48] E. Jentho, C. Ruiz-Moreno, B. Novakovic, I. Kourtzelis, W.L. Megchelenbrink, R. Martins, T. Chavakis, M.P. Soares, L. Kalafati, J. Guerra, F. Roestel, P. Bohm, M. Godmann, T. Grinenko, A. Eugster, M. Beretta, L.A.B. Joosten, M.G. Netea, M. Bauer, H.G. Stunnenberg, S. Weis, Trained Innate Immunity, Long-Lasting Epigenetic Modulation, and Skewed Myelopoiesis by Heme, 2024, https://doi.org/10.1073/pnas.2102698118/-/DCSupplemental.
[49] W.J.M. Mulder, J. Ochando, L.A.B. Joosten, Z.A. Fayad, M.G. Netea, Therapeutic targeting of trained immunity, Nat. Rev. Drug Discov. 18 (2019) 553–566, https://doi.org/10.1038/s41573-019-0025-4.